Journal for Re-Attach Therapy and Developmental Diversities
eISSN: 2589-7799
2023 Sepetember; 6 (9s): 1951-1956

Green Synthesis And Characterization Of Iron And Cobalt Oxide Nanoparticles Using Phaseolus Lunatus Flower Extract

Priyanka Ganesh Bhutekar[1], Anita Kashinath Kshirsagar[2], Shital Shivaji Bankar[3], Sunil Ramrao Mirgane[4*]

Corresponding author email- mirganesunil@gmail.com

[1,2,3,4*]P.G. Department of Chemistry, Jalna Education Society's, R. G. Bagdia Arts, S. B. Lakhotia Commerce, and R. Bezonji Science College, Jalna-431203 (M.S.).

Abstract

Green nanoparticle synthesis is a promising, environmentally friendly, and secure method. Iron oxide nanoparticles (Fe_2O_3-NPs) and cobalt oxide nanoparticles (CoO-NPs) were prepared in the present research by using an aqueous flower extract of phaseolus lunatus. The prepared Fe_2O_3-NPs and CoO-NPs were characterized by ultraviolet-visible spectroscopy, scanning electron microscopy (SEM), dynamic light scattering (DLS), vibrating sample magnetometer (VSM), and differential scanning calorimetry (DSC). The synthesis of FeONPs was validated by the surface plasmon resonance effect. Dynamic light scattering (DLS) showed that the average particle size of FeONPs is around 163.5 nm, with a polydispersity index of 0.091 and a zeta potential of -13.8 mV. Differential scanning calorimetry (DSC) showed an endothermic peak at 176.91°C. The Vibrating Sample Magnetometer (VSM) analysis revealed that iron nanoparticles exhibit superparamagnetic properties with a magnetization value of 3.483 emu/g at room temperature, indicating their potential for use in a magnetically targeted drug delivery system. This biosynthetic approach has been demonstrated to be cost-effective, eco-friendly, and holds great potential for application in biomedical research.

Keywords: Phaseolus Lunatus., Iron Oxide nanoparticle, Cobalt Oxide nanoparticle, Superparamagnetic

1. Introduction:

Nanotechnology is a fast-growing science with many applications in biology, medicine, and technology. Nanotechnology has made significant progress in the realm of nanoscience in the past two decades. Nanotechnology focuses on the production of nanoparticles (NPs) of various shapes and sizes and explores their possible uses [1]. Most experts consider metal oxide nanoparticles to be harmless for both humans and the environment.

Metal oxides are frequently utilized in several domains such as environmental studies, electrochemistry, and magnetic biology [2]. Iron oxide (Fe_2O_3) and cobalt oxide (CoO-NPs) are recognized for their biocompatibility and magnetic properties, making them a favourable metallic nanoparticle for treating specific diseases and infections. Iron oxide nanoparticles (Fe_2O_3NPs) and cobalt oxide nanoparticles (CoO-NPs) are used in various applications such as catalysts, heavy metal adsorption, dyes, and antibiotic degradation [3]. Although the physical and chemical procedures used to synthesize nanoparticles produce well-defined particles, these nanoparticles may not be eco-friendly and are costly. Additionally, utilizing the aforementioned methods to form agglomerates may result in reduced reactivity and stability of these nanoparticles [4]. Recently, the use of plants to synthesize nanomaterials has become popular due to its clean, quick, eco-friendly, and non-toxic nature, with the plant material also acting as a capping agent [5]. The plant's biological components are combined with the NPs, enhancing stability and form [6]. Several recent studies have investigated the eco-friendly production of iron-based nanoparticles using various plant parts like Persea americana rind, Cynometra ramiflora fruit extract, Avicennia marina flower extract, Punica granatum seeds extract, etc., for breaking down various textile dyes [7-11].

The study aimed to prepare iron oxide and cobalt oxide nanoparticles using an extract from the phaseolus lunatus flower. When aqueous ferric chloride and cobalt chloride react with phaseolus lunatus flower extract, it produces very stable Fe_2O_3 and CoO. Nanoparticle synthesis occurs rapidly, enabling the utilization of crop leftovers in the creation of iron nanoparticles by environmentally friendly and safer techniques.

2. Material and Methods

2.1. Materials

Ferrous chloride and cobalt chloride heptahydrate of analytical grade were bought from S. D. Fine, India. The recently harvested phaseolus lunatus flowers were obtained from a local farm.

2.2. Preparation of aqueous leaf extract

Recently harvested phaseolus lunatus flowers were gathered and cleaned with tap water and deionized water. An aqueous extract of the flower was made by mixing 10 g of plant flower (cut into small pieces) with 100 mL of deionized water in

a 250 mL beaker. After heating the solution to 60°C for 1 hour. The mixture was then chilled and filtered with Whatman No. 1 filter paper. The filtrate was centrifuged to obtain a clear solution. A freeze dryer was utilized to dehydrate this transparent extract. The dry powder was sifted through a 60-mesh filter and then stored in an airtight container at room temperature for future experiments.

2.3. Biosynthesis of iron oxide nanoparticles

Iron oxide nanoparticles (Fe_2O_3NPs) were synthesized by slowly adding phaseolus lunatus flower extract to a solution containing 0.01 mM $FeCl_3.7H_2O$ in a 100 mL conical flask while maintaining a constant agitation speed of 1000 rpm. The reaction mixture was stirred for 15 minutes at 30°C using a magnetic stirrer. The iron oxide nanoparticles (Fe_2O_3NPs) were separated using centrifugation at 15000 rpm for 20 minutes. The liquid supernatant was removed, and the solid pellet was purified by washing it with triple distilled water and centrifuging it multiple times. The iron oxide nanoparticles underwent freeze-drying for 24 hours at -78°C under a pressure of 10 Pa. The black pellet was dehydrated and stored for further investigation [12-13].

2.4. Biosynthesis of cobalt oxide nanoparticles

The synthesis of cobalt oxide nanoparticles (CoO-NPs) was accomplished by gradually adding phaseolus lunatus flower extract to a 100 mL conical flask containing a solution of 0.01 mM $CoCl_2.7H_2O$ while keeping the agitation speed constant at 1000 rpm. A magnetic stirrer was used to agitate the reaction mixture for 15 minutes at 30°C. Centrifugation was used for 20 minutes at 15,000 rpm to separate the CoO-NPs. Centrifugation was used several times to remove the liquid supernatant and wash the solid pellet with triple distilled water to purify it. For 24 hours at -78°C and 10 Pa, the iron oxide nanoparticles were freeze-dried. We dehydrated the black pellet and put it away for future research.

2.5. Characterization of synthesized Fe_2O_3-NPs and CoO-NPs:

The synthesis of Fe_2O_3-NPs and CoO-NPs was confirmed using a JASCO V650 UV-vis spectrophotometer. We used SEM (FEI Nova Nano SEM 450) and EDS (Bruker XFlash 6I30) to analyze the size, shape, and elemental composition of Fe_2O_3-NPs and CoO-NPs. A resolution scanning electron microscope was used to analyze the shape and elemental content of the X-ray powder diffraction (XRD) pattern generated by CuK (= 1.5418) in the investigation. The KBr pellet approach was used to obtain FT-IR spectra in the solid phase.

2.6. Antimicrobial Assay:

2.6.1. Antibacterial activity:

Two gram-positive and two gram-negative bacteria were used to test the antibacterial activity of the synthesized Fe_2O_3-NPs and CoO-NPs. Autoclaving the Muller Hilton agar medium at 15 lbs/in^2 for 15 minutes was done for antibacterial testing. Researchers used the disc diffusion technique [14] to find out if the newly synthesized chemicals have antibacterial characteristics. Using sterile distilled water to suspend the culture, the inoculum was reduced to a concentration of around 108 cfu/mL. After 15 minutes of incubation, 20 mL of Muller Hilton agar medium was added to a Petri dish containing swabbed cultures of each microbial strain. The contaminated plates were treated with 100 liters of a 4.0 mg/mL solution of each drug after sterile borers were used to drill 6 mm diameter wells. Each plate was read after incubation for 24 hours at 37 °C. A measurement of the extent of the zone of inhibition surrounding the wells was used to test the antibacterial activity of all synthesized drugs. As a positive control, streptomycin was used, and as a negative control, DMF.

2.6.2. Antifungal Activity:

In a cup-and-plate experiment, the chemicals were examined for their ability to inhibit the growth of two distinct fungal species (C. albicans 1439 and S. cerevisiae MCC1033). Discs with a diameter of 5 mm and a thickness of 1 mm were filled with the test solution using micropipettes. The plates were then placed in an incubator set at 37 °C for 72 hours. This gave the test solution enough time to permeate the medium and influence the pathogens' growth. We were able to determine the size of the inhibitory zone after 36 hours of incubation at 37 °C. The minimal inhibitory doses of compounds that showed promise against fungus were investigated. After incubating an antifungal drug for 24 hours, the minimum inhibitory concentration (MIC) was found to be the lowest dose at which microbial growth was visibly inhibited. To verify microbial resistance to antibiotics and assess the effectiveness of new antibiotics, clinical laboratories used the minimum inhibitory concentration (MIC).

3. Results and Discussion

The Fe_2O_3 and CoO nanoparticles synthesis result was examined and analyzed using conventional equipment and processes in an ecologically conscious manner. The presence of metal oxide nanoparticles was initially identified through a color alteration in the reaction mixture. Interpreting data from UV-vis and FTIR spectra resulted in the synthesis of metal oxide nanoparticles.

3.1. XRD Spectral Analysis:

Optimal experimental circumstances were used to determine the phase purity of the products. The powder XRD patterns of all the iron oxide nanoparticles that were manufactured are displayed in **Figure 1**. The pure hematite Fe_2O_3 phase, which matches completely with PDF-01-077-9926, was detected in the iron oxide. At 33.24°, the primary hematite peak is well visible. The following additional peaks were located and identified: 24.24°, 35.74°, 40.56°, 49.56°, 54.18°, 57.68° (doublet), 62.50°, and 64.12°.

Powder XRD was used to analyze the XRD patterns of samples CoO nanoparticles, which are illustrated in **Figure 1**. The (111), (200), (220), (311), and (222) planes of face-cantered cubic (fcc) CoO are matched with the bulk XRD pattern (CoO, Fm3m, a =4.261 Å, JCPDS #78-0431) in the XRD pattern for sample A, which can be seen at 2θ = 36.36, 44.96, 59.44, 65.30, and 66.00°, respectively. Over the whole angular range of 20-80°, there is no change in the peak position between the experimental and bulk XRD patterns, suggesting that the produced cubic CoO nanocrystals are free of extra strain. The as-synthesized material was determined to be crystalline pure phase CoO with a calculated cell parameter a = 4.262 Å and space group Fm3m, according to detailed structural characterization from X-ray diffraction patterns (obtained through the least-squares refinement of the XRD patterns using the PowderCell program). The synthesized products were confirmed to be of high purity in the XRD pattern, since no additional phases like Co_3O_4, hexagonal β-$Co(OH)_2$, metallic cobalt (Co, JCPDS #05-0727), or hexagonal CoO (JCPDS #80-0075) were observed.

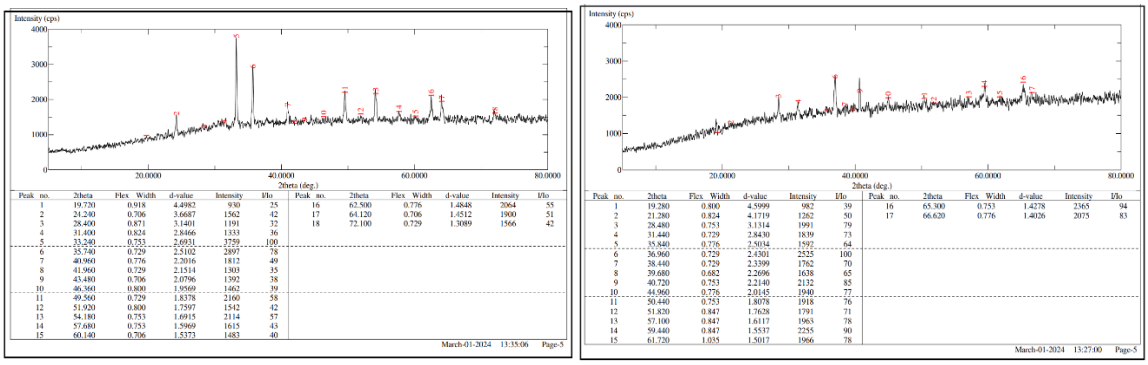

Figure 1: XRD spectra of Fe_2O_3 and CoO NPs

3.2. FT-IR Spectral Analysis:

In the 500-4000 cm^{-1} spectral range, Figure 2 presents the FTIR spectrum of the Fe_2O_3 and CoO NPs. The main bands seen at the region 1553-1633 cm^{-1}, and 1231-1347 cm^{-1} are corresponding to the carbonyl, and functional groups of C-N, respectively, as previously mentioned [71]. The Infrared spectra show two distinct bands at ~667 cm^{-1} and ~577 cm^{-1}, caused by vibration υ(Fe-O and Co-O) modes. These modes are derived from the fingerprint stretching vibrations of the ferric-oxygen and cobalt-oxygen bonds in the Fe_2O_3 and CoO [18].

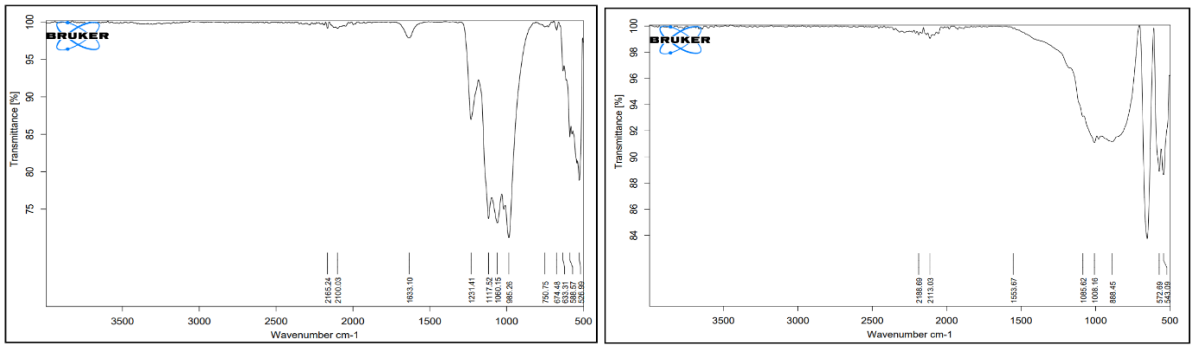

Figure 2: FTIR spectra of Fe_2O_3 and CoO NPs

3.3. UV-Visible Spectral analysis:

Figure 3 displays the UV-visible absorption spectra of pure Fe_2O_3 and CoO nanoparticle samples. The absorption edges occur at wavelengths of 270-273 nm, 339-347 nm, and 345-363 nm. The absorption edges below 400 nm are due to charge transfer from the O; 2p and Fe and Co; 3d states. The absorption spectra of Fe_2O_3 and CoO NPs show a red shift toward higher wavelengths, indicating the transition metal's integration into Fe_2O_3 and CoO NPs lattice sites.

$\alpha h\upsilon = A(h\upsilon - E_g)^n$

The optical band gaps of pure Fe_2O_3 and CoO NPs were determined to be 3.73eV, 3.58eV, and 3.34eV, respectively. Fe_2O_3 and CoO NPs exhibited decreased band gap energy compared to pure Fe_2O_3 and CoO.

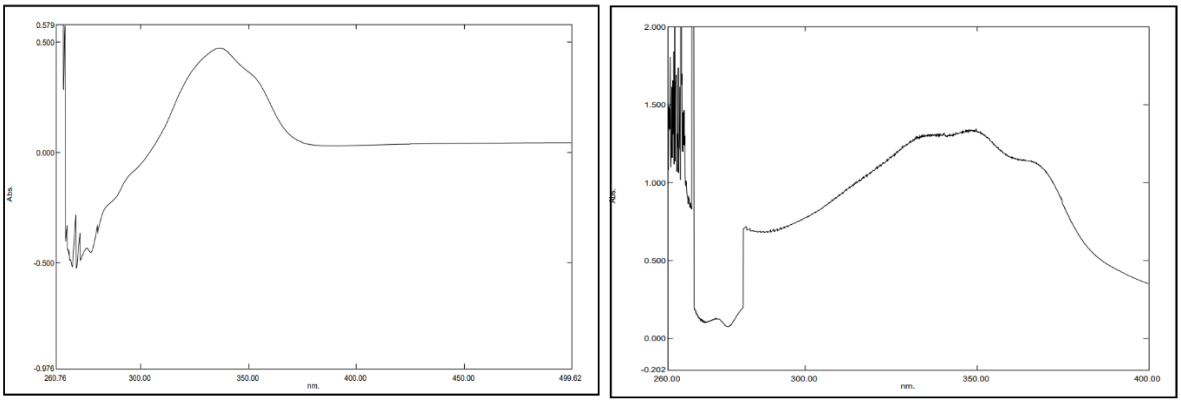

Figure 3. UV-vis spectra of Fe_2O_3 and CoO NPs

3.4. SEM analysis:

The surface structure of pure Fe_2O_3 and CoO nanoparticles can be observed in Figures **4** and **5**. Nanoparticles typically have spherical forms and are on the nanoscale scale. The insertion of Fe ions into the lattice positions of Fe_2O_3 and CoO, respectively, causes the tiny pores in these nanoparticles to enlarge. It was discovered that transition metals could be present.

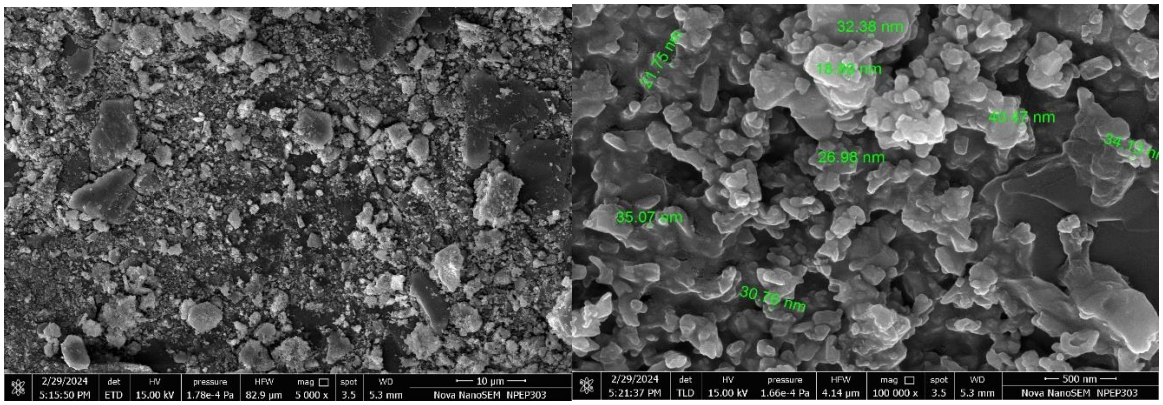

Figure 4: FE-SEM images of Fe_2O_3-NPs with a magnification (10µm and 500nm)

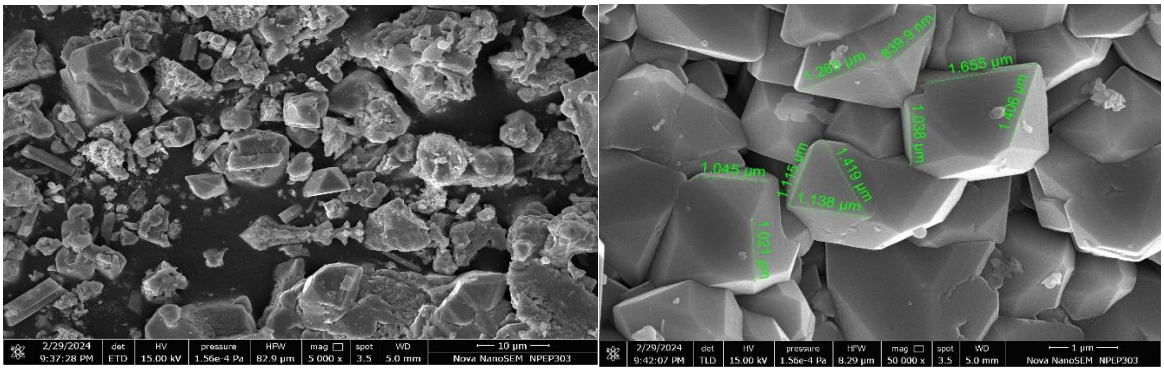

Figure 5: FE-SEM images of CoO-NPs with a magnification (10µm and 500nm).

3.5. EDAX analysis

Nanoparticles of Fe_2O_3 and CoO are analyzed for their elemental makeup in this study. The findings show that the concentration of Fe^{3+} ions is 2.30% and that of Co^{2+} ions is 6.25%. Nanoparticles of iron oxide (Fe_2O_3) and cobalt oxide (CoO) each contain 40% and 60% oxygen atoms, respectively.

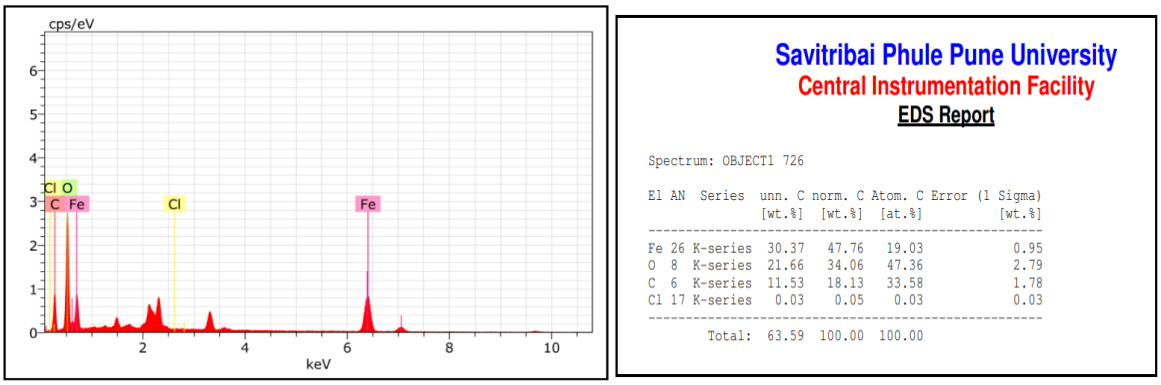

Figure 6: EDAX spectrum for Fe_2O_3-NPs

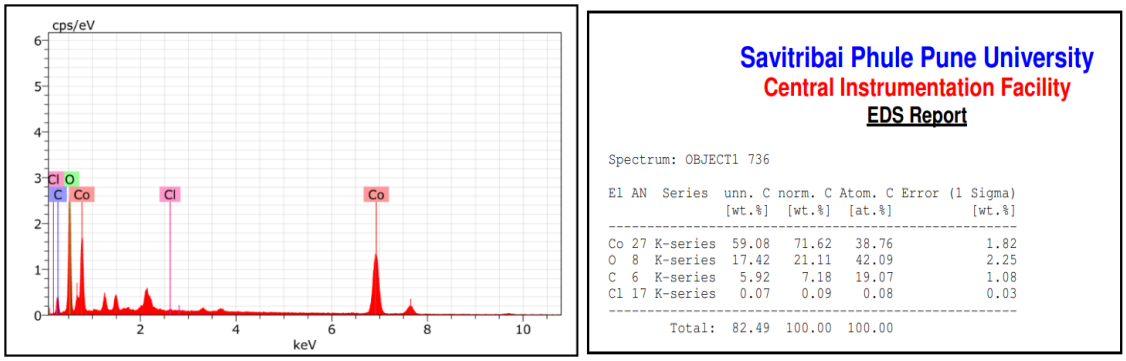

Figure 7: EDAX spectrum for CoO-NPs

3.6. Biological studies:

3.6.1. Antibacterial studies:

In vitro testing was used to evaluate the synthesized Fe_2O_3 and CoO nanoparticle's antibacterial properties against different types of bacteria and fungi. All of the compounds screened for antibacterial activity against S. aureus, B. subtilis, E. coli, and P. aeruginosa exhibited MIC values ranging from 8.2 to 25 mm. The inhibitory values (19.5-24.5 mm) against Staphylococcus aureus were higher for all of the synthesized Fe_2O_3 and CoO nanoparticles compared to streptomycin.

3.6.2. Antifungal studies:

Antifungal studies against two fungi (C. albicans MCC1439 and S. cerevisiae MCC1033) showed that the synthesized compounds were approximately 2.5 times more effective than the reference medication fluconazole (10.5-14.0 mm).

4. Conclusion:

The study shows that Fe_2O_3 and CoO nanoparticles have a face-centered cubic structure and a spherical morphology, as shown by XRD and SEM images. The purity of the elements' composition is confirmed by EDAX analysis. Electron- and metal-oxide nanoparticles effectively kill gram-positive bacteria, including Candida albicans, Staphylococcus cerevisiae, Escherichia coli, and Staphylococcus subtilis. Given that the selected dye shrank in size over time, its catalytic activity was assessed in a solar radiation-containing environment.

Conflict of interest

The authors have no conflicts of interest to declare.

5. References:

1. Darezereshki E, Ranjbar M & Bakhtiari F, One-step synthesis of maghemite (γ- Fe_2O_3) nano-particles by wet chemical method. J Alloys Compd, 502 (2010) 257.
2. Saratale R, Karuppusamy I, Saratale G, Pugazhendhi A, Kumar G & Park Y, A comprehensive review on green nanomaterials using biological systems: recent perception and their future applications. Colloids Surf B: Biointerfaces, 170 (2018) 20.

3. Muthukumar H, Chandrasekaran NI, Mohammed SN, Pichiah S & Manickam M, Iron oxide nano-material: physicochemical traits and in vitro antibacterial propensity against multidrug resistant bacteria. J Ind Eng Chem, 45 (2017) 121.
4. Deepika H, Jacob L & Rajender NN, A greener synthesis of core (Fe, Cu)-Shell (Au, Pt, Pd, and Ag) nanocrystals using aqueous vitamin C. ACS Sustainable Chem Eng, 1 (2013) 703.
5. Oscar LF, Vismaya S, Arunkumar M, Thajuddin N, Dhanasekaran D & Nithya C, Algal nanoparticles: Synthesis and biotechnological potentials.In: Algae- Organisms for Imminent Biotechnology (Ed. by N Thajuddin & D Dhanasekaran, Open Access Peer-reviewed edited volume), 2016.
6. Baker S, Rakshith D, Kavitha KS, Santosh P, Kavitha HU, Rao Y & Satish S, Plants: emerging as nano factories towards facile route in the synthesis of nanoparticles. Bioimpacts, 3 (2013) 111.
7. Makarov VV, Makarova SS, Love AJ, Sinitsyna OV, Dudnik AO, Yaminsky IV, Taliansky ME & Kalinina NO, Biosynthesis of stable iron oxide nanoparticles in aqueous extracts of Hordeum vulgare and Rumex acetosa plants. Langmuir, 30 (2014) 5982.
8. Kamaraj M, Kidane T, Muluken KU & Aravind J, Bio fabrication of iron oxide nanoparticles as a potential photocatalyst for dye degradation with antimicrobial activity. Int J Environ Sci Technol, 16 (2019) 8305.
9. Bishnoi S, Kumar A & Selvaraj R, Facile synthesis of magnetic iron oxide nanoparticles using inedible Cynometra ramiflora fruit extract waste and their photocatalytic degradation of methylene blue dye. Mater Res Bull, 97 (2018) 121.
10. Karpagavinayagam P & Vedhi C,Green synthesis of iron oxide nanoparticles using Avicennia marina flower extract. Vacuum, 160 (2019) 286.
11. Bibi I, Nazar N, Ata S, Sultan M, Ali A, Abbas A, Jilani K, Kamal S, Sarim FM, Khan MI, Jalal F & Iqbal M, Green synthesis of iron oxide nanoparticles using pomegranate seeds extract and photocatalytic activity evaluation for the degradation of textile dye. J Mater Res Technol, 8 (2019) 6115.
12. Safdar, Ammara, Hamza Elsayed Ahmed Mohamed, Khaoula Hkiri, Abdul Muhaymin, and Malik Maaza. "Green Synthesis of Cobalt Oxide Nanoparticles Using Hyphaene thebaica Fruit Extract and Their Photocatalytic Application." Applied Sciences 13, no. 16 (2023): 9082.
13. Chandraker, Sandip Kumar, Mithun Kumar Ghosh, Mishri Lal, Tanmay Kumar Ghorai, and Ravindra Shukla. "Colorimetric sensing of Fe 3+ and Hg 2+ and photocatalytic activity of green synthesized silver nanoparticles from the leaf extract of Sonchus arvensis L." New Journal of Chemistry 43, no. 46 (2019): 18175-18183.
14. Abdi, Mohammed, Zekeria Yusuf, and J. M. Sasikumar. "Phyto-fabrication of Cobalt Oxide Nanoparticles from L. Leaf and Flower Extracts and their Antimicrobial Activities." The Open Biotechnology Journal 17, no. 1 (2023).
15. Jemilugba, Olufunto T., Sundararajan Parani, Vuyo Mavumengwana, and Oluwatobi S. Oluwafemi. "Green synthesis of silver nanoparticles using Combretum erythrophyllum leaves and its antibacterial activities." Colloid and interface science communications 31 (2019): 100191.
16. Anuradha, C. T., and P. Raji. "Facile-synthesis and characterization of cobalt oxide (Co3O4) nanoparticles by using Arishta leaves assisted biological molecules and its antibacterial and antifungal activities." Journal of Molecular Structure 1262 (2022): 133065.
17. Renuga, D., J. Jeyasundari, AS Shakthi Athithan, and Y. Brightson Arul Jacob. "Synthesis and characterization of copper oxide nanoparticles using Brassica oleracea var. italic extract for its antifungal application." Materials Research Express 7, no. 4 (2020): 045007.
18. Asha, G., V. Rajeshwari, G. Stephen, S. Gurusamy, and D. Carolin Jeniba Rachel. "Eco-friendly synthesis and characterization of cobalt oxide nanoparticles by sativum species and its photo-catalytic activity." Materials Today: Proceedings 48 (2022): 486-493.